




ABRUPT INCREASE OF RADIOCARBON CONCENTRATION IN 660 BC IN TREE RINGS FROM GRABIE NEAR KRAKÓW (SE POLAND)

Andrzej Rakowski^{1*}  • Marek Krapiec² • Matthias Huels³  • Jacek Pawlyta¹  • Christian Hamann³ • Damian Wiktorowski²

¹Institute of Physics - Center for Science and Education, Silesian University of Technology, Konarskiego 22B str., 44-100 Gliwice, Poland

²AGH University of Science and Technology, Mickiewicza Av. 30, 30-059 Krakow, Poland

³Leibniz-Laboratory for Radiometric Dating and Isotope Research, University Kiel, Max-Eyth-Str. 11-13, 24118 Kiel, Germany

ABSTRACT. Miyake et al. (2012, 2013, 2014) described a sudden increase of radiocarbon (¹⁴C) concentration in annual tree rings of Japanese cedar (*Cryptomeria japonica*) and Hinoki cypress (*Chamaecyparis obtusa*) between AD 774 and 775 and between AD 993 and 994. In both analyzed periods, the sudden increase was observed almost in a single year. The increase in the ¹⁴C content was about 12‰ in the period AD 774–775 (Miyake et al. 2012) and about 11.3‰ in the period AD 993–994 (Miyake et al. 2013, 2014; Fogtmann-Schultz et al. 2017; Rakowski et al. 2018). A similar increase was observed in 660 BC, with a peak height of about 10‰ (Park et al. 2017). Single-year samples of dendrochronologically dated tree rings of deciduous oak (*Quercus robur*) from Grabie, a village near Krakow (SE Poland), spanning the years 670–652 BC, were collected and their ¹⁴C content was measured using an AMS technique. The results clearly show a rapid increase in the ¹⁴C concentration in tree rings around 660 BC similar to this observed in Park et al. (2017).

KEYWORDS: AMS, atmosphere, biosphere, calibration curve, cosmogenic isotopes, Miyake effect, radiocarbon, tree rings.

INTRODUCTION

Radiocarbon (¹⁴C) is a cosmogenic radioisotope continuously produced in the Earth's atmosphere due to nuclear reaction ¹⁴N(n,p)¹⁴C. In the next step the new formed radioisotope is oxidized to produce ¹⁴CO₂, and in this form through many different processes is incorporated into the global carbon cycle. Plants incorporate ¹⁴CO₂ due to photosynthesis, and ¹⁴C concentration in biogenic material reflects its concentration in the atmosphere during the growing season.

The production rate changes with latitude and depends on the intensity of the cosmic ray flux and the global average value is in order of 2 atoms·cm⁻²·s⁻¹ (Castagnoli and Lal 1980; Kvaltsov et al. 2012). Natural changes in the intensity of solar, interplanetary and Earth's magnetic field are the main factors modulating the intensity of cosmic ray flux reaching the Earth's atmosphere. The extraterrestrial high-energy events, such as solar proton events (SPEs), supernovae explosions (SNe), gamma-ray bursts (GRBs), have a significant impact on the ¹⁴C production rate. Such phenomena lead to a short-term increase in ¹⁴C concentration in the atmosphere, and through carbon exchange mechanisms, in other carbon reservoirs, and can be observed i.e. in annual tree rings.

Miyake et al. (2012) were the first to describe sharp and short-lasting increase of ¹⁴C (¹⁴C) concentration in the annual tree rings of the Japanese cedar (*Cryptomeria japonica*) between AD 774/775. The increase of ¹⁴C concentration for this event (henceforth M12) was about 12‰ between AD 774 and 775, and has been confirmed by several authors (Jull et al. 2014; Güttler et al. 2015; Rakowski et al. 2015; Büntgen et al. 2018). Results from samples of annual tree rings from Siberia (Jull et al. 2014) indicate that the increase of ¹⁴C concentration in the atmosphere already began in AD 774, and continued to AD 776. This

*Corresponding author. Email: arakowski@polsl.pl.

suggests that the reason for the increase in ^{14}C concentration was not a single phenomenon, but rather a series of similar phenomena occurring over a longer period of time. The maximum ^{14}C concentration for this event recorded in samples of the kauri tree (*Agathis australis*) from New Zealand is observed half a year later (Güttler et al. 2015), probably due to the Southern Hemisphere offset (Rodgers et al. 2011).

Since then, other events similar to the M12 have been observed at various time intervals. Miyake et al. (2013, 2014) have observed another rapid increase of ^{14}C content between 9.1‰ and 11.3‰ in the period AD 993–994. This has also been confirmed by other research teams (Fogtmann-Schultz et al. 2017; Rakowski et al. 2018). Park et al. (2017) have reported such event around 660 BC, Jull et al. (2018) observed ^{14}C increase at 814–815 BC, Wang et al. (2017) have observed rapid increase of ^{14}C concentration at 3372–3371 BC, and Miyake et al. (2017) have found a large ^{14}C excursion in mid-Holocene around 5480 BC.

Based on the calculation of ^{14}C production rate for the M12 event, Miyake et al. (2012) made a first attempt to explain the possible causes of this phenomena. The ^{14}C production rate $6 \cdot 10^8$ atoms $\cdot\text{cm}^{-2}$, obtained for this event by applying four-box carbon cycle model, is very high, and could be explain only by a giant solar eruption or supernovae explosion. Since there is no evidence for SNe in this period of time, this possibility can be ignored. Using another carbon cycle model (5-box model), Usoskin et al. (2013) had recalculated the ^{14}C production rate for this event. The value obtained $(1.3 \pm 0.2) \cdot 10^8$ atoms $\cdot\text{cm}^{-2}$ is around 4 times smaller than presented in Miyake et al. (2012). This discrepancy was later explained (Miyake et al. 2014) as due to calculation error. The production rate for the Miyake event at AD 993/994 is smaller and has value $(0.9 \pm 0.2) \cdot 10^8$ atoms $\cdot\text{cm}^{-2}$ (Miyake et al. 2014). The ^{10}Be and ^{36}Cl measurements in ice core from Antarctica and Greenland also show a spike around AD 775 and AD 994, which indicates a large SEP or series of SEP as a potential cause of those events (Mekhaldi et al. 2015). Typical GRB energy spectra and fluxes could generate significant amounts of ^{14}C , however, they would not significantly affect ^{10}Be production rate (Pavlov et al. 2013; Mekhaldi et al. 2015).

Here, we report the measurement of ^{14}C concentration along with stable isotopic composition of carbon, for a sub-fossil oak (*Quercus robur*) from southern Poland for the period 670–650 BC to search for increase in ^{14}C concentration due to a Miyake effect.

SAMPLE AND METHODS

Sub-fossil oaks (*Quercus robur* L.) were recovered from a site in a gravel pit by the Vistula river in the village of Grabie, near Krakow (50.0391 N, 19.992 E; Figure 1). Slices of 100 oak trunks were taken for dendrochronological studies. After sample preparation to disclose visible anatomic structure and enable identification of annual growth rings, measurement tracks along 2–4 trunk radii were delineated. Measurements were made with 0.01 mm accuracy using a DENDROLAB 1.0 apparatus, then the ring-width sequences were processed with a set of computer programs TREE-RINGS (Krawczyk and Krapiec 1995), TSAP (Rinn 2005) and DPL (Holmes 1999).

The oaks from Grabie were felled at inundations in the Vistula river valley within the last two millennia BC. As some of them were long-lived, 300–400 year-old trees, two standards could be produced, which spanned the years 1750–1018 BC (chronology GAA_1U) and 994–612 BC (chronology GAA_3U) (Krapiec 2001). Sample G58 was selected for ^{14}C analysis, spans BC 797–620, dendrochronologically-dated using the standard for southern Poland oak, C_3000E (Krapiec 2001) with $t = 15.5$, $\text{GL} = 79\%$, where the t -value represents the significance of the



Figure 1 Location of Grabie village (50.0391 N, 19.992 E).

correlation of two series in relations to their overlap and should not drop to a value below 3.5 (Baillie and Pilcher 1973). The GL was developed as a special tool for cross-dating of tree-ring series. The degree of similarity based on the positive or negative trend of each width is expressed as a percentage of the number of intervals (Eckstein and Bauch 1969).

Each annual tree ring from 670–650 BC was washed in distilled water, and α -cellulose was extracted using the Green (1963) protocol with some modifications. To accelerate the separation of single cellulose fibers from wood samples, and thus to increase the penetration of reagents, an ultrasonic bath was utilized (Michczyńska et al. 2018). Wood samples were dried and cut into shavings, then weighed and placed into glass tubes. Each sample was putted into glass tube with deionized water, sodium chlorite, and 1% HCl. The tube was then placed in an ultrasonic bath kept at 70°C for 1 hr, and then sodium chlorite and 1% HCl was added to each sample. This procedure was repeated five times, and the samples were then rinsed with hot deionized water up to neutral pH. This process removes most of the lignin and the remaining sample consists mostly of holocellulose. For the next step, 10% NaOH solution was added to the samples and then put into an ultrasonic bath at 70°C for 45 min. After the solution was removed, the sample was rinsed with cold deionizing water. Next, 17% NaOH solution was added and samples were put into ultrasonic bath at room temperature for 45 min. After this time deionizing water was added to the samples. This step removes rest of the remaining lignin and holocellulose. The sample were then rinsed with hot deionized water up to neutral pH. Finally, 1% HCl was added to the samples and the samples were rinsed to neutral pH. The obtained α -cellulose was dried overnight at 70°C.

About 4 mg of α -cellulose extracted from each sample was transferred into a prebaked (900°C) quartz ampoules together with CuO and Ag, evacuated to a pressure of 10^{-5} mbar, sealed and combusted for 4 hr at 900°C in a muffle oven (Krapiec et al. 2018). The resulting CO₂ was released under vacuum and cryogenically purified for subsequent graphitization during the reaction with H₂ at 600°C, on an Fe catalyst (Nadeau et al. 1998).

The resulting mixture of graphite and Fe powder was pressed into a target holder for AMS ¹⁴C measurements. All prepared targets contain approximately 1 mg of carbon and were measured at either the Leibniz-Laboratory of the University of Kiel (Labcode KIA, Nadeau et al. 1998) or the Center for Applied Isotope Studies at the University of Georgia, USA (Labcode UGAMS; Cherkinsky et al. 2010), respectively. The possible offset between those two AMS laboratories has been checked before and the results were presented in Krapiec et al. (2018). ¹⁴C contents are reported as $\Delta^{14}\text{C}$ in per mil (‰) deviations from the standard sample, 0.7459 activity of NBS oxalic acid (SRM-4990C). Age correction and isotopic compositions correction were calculated following formulas presented in (Stuiver and Polach, 1977). The correction for isotopic composition was made based on $\delta^{13}\text{C}$ measured with AMS system. The age calculation was presented in Nadeau and Grootes (2013).

$\delta^{13}\text{C}$ was measured in the subsamples of the same alpha-cellulose extracted for the need of ¹⁴C measurements. Composition of stable carbon isotopes was determined using Eurovector 3000 elemental analyzer (Eurovector Srl, Italy) coupled with IsoPrime isotope ratio mass spectrometer (Elementar UK Ltd.). 110–130 μg of α -cellulose, which gives about 60 μg of carbon, was weighed for each sample and packed in a tin capsule. The tin wrapped samples were combusted in the reactor set to 1030°C temperature in the excess of oxygen. Because of the oxidation of tin wrapping in the reactor, effective combustion temperature was a couple of hundreds of centigrade higher. Resulting gases were passing through Cu-filled reactor operating at 650°C and dried in the magnesium perchlorate filled water trap. Gases were then separated in a packed chromatographic column and transferred in a helium stream to open-split interface of IsoPrime. IRMS was working in a continuous-flow mode. IAEA-C3 cellulose sample (IAEA 2014) was used as a reference material, B2213 spruce powder certified material (Elemental Microanalysis Ltd) and WSTA wheat sample (Boettger et al. 2007) were used to check both stability of the EA-CF-IRMS system and isotopic delta calculations. $\delta^{13}\text{C}$ values were expressed in ‰ versus VPDB scale (Coplen et al. 2006). Samples were randomized in the measurement queue in order to minimize instrument drift effect on the time series data. Uncertainty of $\delta^{13}\text{C}$ was estimated as a standard deviation of repeated monitoring/standard sample measurements.

RESULTS AND DISCUSSION

The measured results ($F^{14}\text{C}$, $\Delta^{14}\text{C}$, and $\delta^{13}\text{C}$) with corresponding uncertainties are presented in Table 1. Figures 2 and 3 show $\Delta^{14}\text{C}$ and $\delta^{13}\text{C}$ for the period 670–652 BC. The series G58 has been measured at Leibniz Laboratory of the University of Kiel, except for two samples (G58-7 and G58-8), which have been measured at the Center for Applied Isotope Studies at the University of Georgia, USA.

On the broad scale, the Grabie tree rings sequence between 670 BC and 652 BC showed a similar pattern to that seen in German oak reported by Park et al. (2017). We observed a gradual increase in $\Delta^{14}\text{C}$ of $18.2 \pm 3.6\text{‰}$ (p-value for the t-Student test of the increase is equal 0.055) from 665 BC ($\Delta^{14}\text{C} = -3.1 \pm 2.2\text{‰}$) to 662 BC ($\Delta^{14}\text{C} = 15.1 \pm 2.8\text{‰}$). In the

Table 1 $F^{14}\text{C}$, $\Delta^{14}\text{C}$, and $\delta^{13}\text{C}_{\text{PDB}}$ values for annual tree rings of *Quercus robur* from Grabie village near Kraków (SE Poland). Uncertainty of $\delta^{13}\text{C}_{\text{IRMS}}$ measurements was estimated as 0.20‰.

Sample	Year BC	Lab ID	$F^{14}\text{C}$	$\Delta^{14}\text{C}(\text{‰})$	$\delta^{13}\text{C}_{\text{IRMS}}$ (‰VPDB)
G58-1	670	KIA-52778	0.7336 ± 0.0022	7.2 ± 2.2	-26.84
G58-2	669	KIA-52779	0.7335 ± 0.0022	7.1 ± 2.2	-25.71
G58-3	668	KIA-52780	0.7279 ± 0.0021	-0.8 ± 2.1	-26.23
G58-4	667	KIA-52781	0.7296 ± 0.0022	1.4 ± 2.2	-25.70
G58-5	666	KIA-52782	0.7277 ± 0.0023	-1.3 ± 2.3	-25.77
G58-6	665	KIA-52783	0.7265 ± 0.0022	-3.1 ± 2.2	-26.47
G58-7	664	UGAMS-35617	0.7327 ± 0.0019	5.2 ± 1.9	-25.21
G58-8	663	UGAMS-35618	0.7324 ± 0.0019	4.8 ± 1.9	-25.36
G58-9	662	KIA-52786	0.7400 ± 0.0028	15.1 ± 2.8	-25.32
G58-10	661	KIA-52787	0.7409 ± 0.0026	16.2 ± 2.6	-25.46
G58-11	660	KIA-52788	0.7410 ± 0.0022	16.1 ± 2.2	-25.51
G58-12	659	KIA-52789	0.7408 ± 0.0026	15.7 ± 2.6	-24.75
G58-13	658	KIA-52790	—	—	-24.31
G58-14	657	KIA-52791	0.7360 ± 0.0025	8.9 ± 2.5	-24.46
G58-15	656	KIA-52792	—	—	-24.17
G58-16	655	KIA-52793	0.7371 ± 0.0027	10.1 ± 2.7	-25.14
G58-17	654	KIA-52794	0.7321 ± 0.0022	3.2 ± 2.2	-25.08
G58-18	653	KIA-52795	—	—	-24.76
G58-19	652	KIA-52796	0.7403 ± 0.0025	14.1 ± 2.5	-24.19
G58-20	651	KIA-52797	—	—	-24.43
G58-21	650	KIA-52798	—	—	-24.02

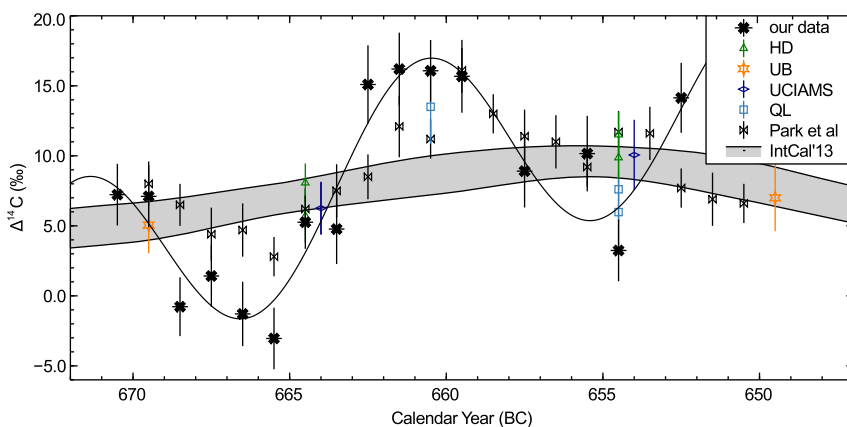
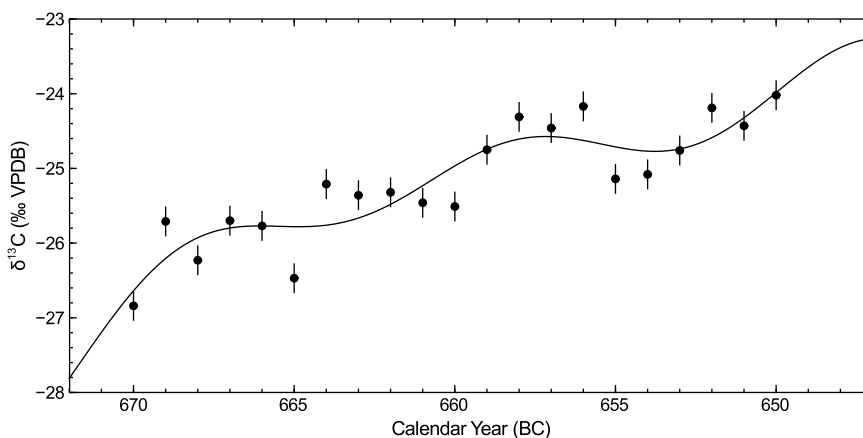


Figure 2 $\Delta^{14}\text{C}$ time series for G58 core (crosses) with a fitted sum of three periodic functions (smooth line), IntCal13 (grey-shaded area) (Reimer et al. 2013), Park et al. (2017) data (double empty triangle) and raw atmospheric data (empty triangles, empty stars, empty diamonds, and empty rectangles). Raw datasets named as in the database (IntCal13 2013) Parameters of fit are presented in the Table 2.

Table 2 Parameters of the sum of three periodic function fitting to the $\Delta^{14}\text{C}$ time series and $\delta^{13}\text{C}$ time series.

Parameter	Value	Unit
	$T_1 = 11$ yr	
A_1	7.2 ± 1.3	‰
ϕ_{A1}	645.51 ± 0.41	BC
	$T_2 = 22$ yr	
A_2	0.3 ± 1.4	‰
ϕ_{A2}	641 ± 45	BC
	$T_3 = 88$ yr	
A_3	13.2 ± 5.9	‰
ϕ_{A3}	647.0 ± 4.0	BC
$\delta^{13}\text{C}$	-28 ± 11	‰ VPDB
	$T_1 = 11$ yr	
δ_1	0.38 ± 0.21	‰
ϕ_1	660.6 ± 1.4	BC
	$T_2 = 22$ yr	
δ_2	0.48 ± 0.62	‰
ϕ_2	650.4 ± 9.5	BC
	$T_3 = 88$ yr	
δ_3	3.8 ± 9.1	‰
ϕ_3	672 ± 30	BC

Figure 3 $\delta^{13}\text{C}$ time series for G58 core (dots) with a fitted sum of three periodic functions and a constant value. Parameters of fit are presented in the Table 2.

first step, we observed an increase in $\Delta^{14}\text{C}$ to $\sim 5.2\text{‰}$ ($\Delta^{14}\text{C}$ increase of $8.3 \pm 2.9\text{‰}$) between 665 and 664 BC, followed by a second jump in $\Delta^{14}\text{C}$ to $\sim 15.1\text{‰}$ ($\Delta^{14}\text{C}$ increase of $10.3 \pm 3.4\text{‰}$) between 663 and 662 BC. After 662 BC, the high level of ^{14}C concentration ($\Delta^{14}\text{C} \sim 16\text{‰}$) lasted for the next several years until 659 BC, and then began to decrease. At the end of the analyzing period at 652 BC, we observed an increase in $\Delta^{14}\text{C}$ to $14.1 \pm 2.5\text{‰}$, however without precise measurements around this period it is difficult to conclude the

reason for such a high value. We found that $\Delta^{14}\text{C}$ time series may be quite well described as a sum of three periodic functions above a constant level.

The sum of three periodic functions: $\Delta_i(t) = A_i \sin(2 \cdot \pi \cdot t / T_i + 2 \cdot \pi \cdot \varphi_{A_i} / T_i)$ was fitted to the $\Delta^{14}\text{C}$ time series. Levenberg-Marquardt routine from mpfit library version 1.3 and Fityk version 1.3.1 software (Wojdyr 2010) were used for periodic function fitting. T_i were chosen arbitrary to reflect three main observed Sun periodicities: 11, 22, and 88 yr (Usoskin 2017, Peristykh and Damon 2003). Similarly, an attempt was made to fit the sum of three periodic functions: $\delta^{13}\text{C}(t) = \delta_i \sin(2 \cdot \pi \cdot t / T_i + 2 \cdot \pi \cdot \varphi_i / T_i)$ plus a constant value to $\delta^{13}\text{C}$ time series. Local maxima and minima for fitted functions for the period ranging from 700 BC to 600 BC were found using Scilab version 6.01 software.

Results of the periodic functions fitting are given in Table 2 and in Figure 2. The maximum of the fitted functions to the $\Delta^{14}\text{C}$ time series in the time range from 700 BC to 600 BC is equal 20.71‰ (for 648.8 BC) while minimum is equal to -19.64 ‰ (for 699.2 BC). The estimated amplitude of the semi-periodic fluctuations fitted to $\Delta^{14}\text{C}$ data is equal to about 20‰. Most of the $\Delta^{14}\text{C}$ fluctuations (about 13‰) may be explained by 88-yr solar cycle (Table 2), up to about 7.2‰ may be described by 11-yr cycle. Influence of the 11-yr cycle on the fluctuations is small (less than 0.3‰).

The results of our previous studies regarding the Miyake effect in AD 774/775 (Rakowski et al. 2015) and AD 993/994 (Rakowski et al. 2018) also indicated that they are a consequence of elevated solar activity. Similar to the results obtained for this study, our previous results also show an increase in ^{14}C concentration, which took place gradually over several consecutive years. Park et al. (2017) suggested that a combination of coronal mass ejection events (CME) and associated SPEs could have been a common cause for Miyake events around 660BC, AD 774/775 and AD 993/994. Single-year data and decadal data (from different places) included in IntCal13 (Reimer et al. 2013) show also rapid increase in ^{14}C concentration around 660 BC, which suggests that this effect, similar to Miyake effects in AD 774/775 and AD 993/994, has a global character.

Increased solar activity, in addition to increased production of ^{14}C and other cosmogenic isotopes, can directly affect the climate on the Earth. The results of study by Calisto et al. (2012) suggest that even smaller SEPs observed in 1859 (Carrington event; Clauer and Sicoe 2006) could lead to ozone depletion in atmosphere and to significant climate cooling. If such an effect occurred, it may be visible in stable isotopes composition of carbon and oxygen in cellulose from tree rings.

CONCLUSIONS

The results of our study confirm that the abrupt increase in ^{14}C concentration around 660 BC is shown in annual tree rings of oak (*Quercus robur*) from southern Poland. The rapid increase in $\Delta^{14}\text{C}$ between 663 and 662 BC of 10.3 ± 3.4 ‰ corresponds well with value reported by Park et al. (2017). Also, the IntCal13 curve (Reimer et al. 2013) shows a large excursion in ^{14}C concentration around this period. Those data have been obtained from annual rings of trees growing in different locations. This support the hypothesis that we dealing with global phenomena that has its sources in changes in the solar activity. The identification of such events is of great use for precise dating, for example by using the wiggle-match method. The $\delta^{13}\text{C}$ data does not show clear periodic fluctuations, which suggests that these particular changes of solar activity did not induce abrupt climatic changes.

ACKNOWLEDGMENTS

We express our thanks to all the staff of the Radiocarbon Laboratory of Silesian University of Technology for their kind support. This work was supported by National Science Centre, Poland, grant UMO-2017/25/B/ST10/02329 and partly by AGH grant 11.11.140.005.

REFERENCES

- Baillie MGL, Pilcher JR. 1973. A simple crossdating program for tree-ring research. *Tree-Ring Bulletin* 33:7–14.
- Boettger T, Haupt M, Knöller K, Weise SM, Waterhouse JS, Rinne KT, Loader NJ, Sonninen E, Jungner H, Masson-Delmotte V, Stievenard M, Guillemain M-T, Pierre M, Pazdur A, Leuenberger M, Flot M, Saurer M, Reynolds CE, Helle G, Schleser GH. 2007. Wood cellulose preparation methods and mass spectrometric analyses of $\delta^{13}\text{C}$, $\delta^{18}\text{O}$, and nonexchangeable $\delta^2\text{H}$ values in cellulose, sugar, and starch: an interlaboratory comparison. *Analytical Chemistry* 79:4603–4612. doi: [10.1021/ac0700023](https://doi.org/10.1021/ac0700023)
- Büntgen U, Wacker L, Galván JD, Arnold S, Arseneault D, Baillie M, Beer J, Bernabei M, Bleicher N, Boswijk G, et al. 2018. Tree rings reveal globally coherent signature of cosmogenic radiocarbon events in 774 and 993 CE. *Nature Communications* 9(1):3605. doi: [10.1038/s4167-018-06036-0](https://doi.org/10.1038/s4167-018-06036-0).
- Calisto M, Verronen PT, Rozanov E, Peter T. 2012. Influence of a Carrington-like event on the atmospheric chemistry, temperature and dynamics. *Atmos. Chem. Phys.* 12:8679–8686.
- Castagnoli G, Lal D. 1980. Solar modulation effects in terrestrial production of carbon-14. *Radiocarbon* 22:133–158.
- Coplen TB., et al. 2006. New guidelines for $\delta^{13}\text{C}$ measurements. *Anal. Chem.* 78:2439–2441.
- Cherkinsky A, Culp RA, Dvoracek DK, Noakes JE. 2010. Status of the AMS facility at the University of Georgia. *Nuclear Instruments and Methods in Physics Research B* 268(7–8):867–870.
- Clauer CR, Siscoe G, editors. 2006. The great historical geomagnetic storm of 1859: a modern look. *Adv. Spec. Res.* 38:115–388.
- Coplen TB, Brand WA, Gehre M, Gröning M, Meijer HAJ, Toman B, Verkouteren RM, 2006. New guidelines for $\delta^{13}\text{C}$ measurements. *Analytical Chemistry* 78:2439–2441. doi: [10.1021/ac052027c](https://doi.org/10.1021/ac052027c)
- Eckstein D, Bauch J. 1969. Beitrag zur Rationalisierung eines dendrochronologischen Verfahrens und zur Analyse seiner Aussagesicherheit. *Forstwissenschaftliches Centralblatt* 88:230–250.
- Fogtmann-Schulz A, Ostbo SM, Nielsen SGB, Olsen J, Karoff C, Knudsen MF 2017. Cosmic ray event in 994 CE recorded in radiocarbon from Danish oak. *Geophysical Research Letters* 44(16):8621–8628.
- Green JW. 1963. Methods of carbohydrate chemistry. In: Whistler RL, editor. *Methods in carbohydrate chemistry*. New York: Academic Press. p 9–21.
- Güttler D, Adolphi F, Beer J, Bleicher N, Boswijk G, Christl M, Hogg A, Palmer J, Vockenhuber C, Wacker L, Wunder J. 2015. Rapid increase in cosmogenic ^{14}C in AD 775 measured in New Zealand kauri trees indicates short-lived increase in ^{14}C production spanning both hemispheres. *Earth and Planetary Science Letters* 411:290–297.
- Holmes RL, 1999. Users manual for program COFECHA. Tucson (AZ): University of Arizona.
- IAEA. 2014. Materials with known ^2H , ^{13}C , ^{15}N and ^{18}O isotopic composition, IAEA-CH-3 cellulose; [accessed 2014 Apr 24]. http://nucleus.iaea.org/rpst/ReferenceProducts/ReferenceMaterials/Stable_Isotopes/2H13C15Nand18O/IAEA-CH-3.htm.
- IntCal13 Data Sets. 2013. [accessed 2018 Dec 23]. <http://intcal.qub.ac.uk/intcal13/>.
- Jull AJT, Panyushkina IP, Lange TE, Kukarskih VV, Myglan VS, Clark KJ, Salzer MW, Burr GS, Leavitt SW. 2014. Excursions in the ^{14}C record at A.D. 774–775 in tree rings from Russia and America. *Geophysical Research Letters* 41(8):3004–10
- Jull AJT, Panyushkina I, Miyake F, Masuda K, Nakamura T, Mitsutani T, Lange TE, Cruz R, Baisan C, Janovics R, Varga T, Molnar M. 2018. More rapid ^{14}C excursions in the tree-ring record: A record of different kind of solar activity at about 800 BC? *Radiocarbon* 60(4):1237–1248.
- Kovaltsov GA, Mishev A, Usoskin IG. 2012. A new model of cosmogenic production of radiocarbon ^{14}C in the atmosphere. *Earth and Planetary Science Letters* 337–338:114–120.
- Krawczyk A and Krapiec M, 1995. Dendrochronologiczna baza danych. Materiały II Krajowej Konferencji: Komputerowe wspomaganie badań naukowych (Dendrochronological database. Proceedings of the Second Polish Conference on Computer Assistance to Scientific Research). Wrocław: 247–52. In Polish.
- Krapiec M, 2001. Holocene dendrochronological standards for subfossil oaks from the area of Southern Poland. *Studia Quaternaria* 18: 47–63.
- Krapiec M, Rakowski AZ, Huels M, Wiktorowski D, Hamann C. 2018. A new graphitization system for radiocarbon dating with AMS on the

- dendrochronological laboratory at AGH-UST Kraków. *Radiocarbon* 60(4):1091–1100. doi: [10.1017/rde.2018.60](https://doi.org/10.1017/rde.2018.60).
- Mekhaldi F, Muscheler R, Adolphi F, Aldahan A, Beer J, McConnell JR, Possnert G, Sigl M, Svensson A, Synal H-A, Welten KC, Woodruff TE. 2015. Multiradionuclide evidence for the solar origin of the cosmic-ray events of AD 774/5 and 993/4. *Nature Communications* 6: 8611.
- Michczyńska DJ, Krapiec M, Michczyński A, Pawlyta J, Goslar T, Nawrocka N, Piotrowska N, Szychowska-Krapiec E, Waliszewska B, Zborowska M. 2018. Different pretreatment methods for ^{14}C dating of Younger Dryas and Allerød pine wood (*Pinus sylvestris* L.). *Quaternary Geochronology* 48:38–44.
- Miyake F, Nagaya K, Masuda K, Nakamura T. 2012. A signature of cosmic-ray increase in AD 774–775 from tree rings in Japan. *Nature* 486(7402):240–242.
- Miyake F, Masuda K, Nakamura T. 2013. Another rapid event in the carbon-14 content of tree rings. *Nature Communications* 4:1748. doi: [10.1038/ncomms2873](https://doi.org/10.1038/ncomms2873).
- Miyake F, Masuda K, Hakozaiki M, Nakamura T, Tokanai F, Kato K, Kimura K, Mitsutani T. 2014. Verification of the cosmic-ray event in AD 993–994 by using a Japanese Hinoki tree. *Radiocarbon* 56(3):1184–1194.
- Miyake F, Jull AJT, Panyushkina IP, Wacker L, Salzer M, Baisan CH, Lange T, Cruz R, Masuda K, Nakamura T. 2017. Lagrge ^{14}C excursion in 5480 BC indicates an abnormal sun in the mid-Holocene. *Proceedings of the National Academy of Sciences of the United States of America* 114(5):881–884. doi: [10.1073/pnas.1613144114](https://doi.org/10.1073/pnas.1613144114).
- Nadeau M-J, Grootes PM, Schleicher M, Hasselberg P, Rieck A, Bitterling M. 1998. Sample throughput and data quality at the Leibniz-Labor AMS facility. *Radiocarbon* 40(1):239–246.
- Nadeau M-J, Grootes PM. 2013. Calculation of the compounded uncertainty of ^{14}C AMS measurements. *Nuclear Instruments and Methods in Physics Research* 294:420–425.
- Park J, Southon J, Fahrni S, Creasman PP, Mewaldt R. 2017. Relationship between solar activity and $\Delta^{14}\text{C}$ peaks in AD 775, AD 994, and 660 BC. *Radiocarbon* 59(4):1147–1156.
- Pavlov A, Blinov AV, Konstantinov AN, Ostryakov VN, Vasilyev GI, Vdovina MA, Volkov PA. 2013. AD 775 pulse of cosmogenic radionuclides production as imprint of a Galactic gamma-ray burst. *Mon. Not. R. Astron. Soc.* 435(4): 2878–2884.
- Peristykh AN, Damon PE. 2003. Persistence of the Gleissberg 88-year solar cycle over the last ~12, 000 years: evidence from cosmogenic isotopes. *Journal of Geophysical Research: Space Physics* 108(A1): 1003. doi: [10.1029/2002JA009390](https://doi.org/10.1029/2002JA009390).
- Reimer PJ, Bard E, Bayliss A, Beck WJ, Blackwell PG, Bronk Ramsey C, Buck CE, Cheng H, Edwards RL, Friedrich M, Grootes PM, Guilderson TP, Hafflidason H, Hajdas I, Hatté C, Heaton TJ, Hoffman DL, Hogg AG, Hughen KA, Kaiser KF, Kromer B, Manning SW, Niu M, Reimer RW, Richards DA, Scott EM, Southon JR, Staff RA, Turney CSM, van der Plicht J. 2013. IntCal13 and Marine13 radiocarbon age calibration curves 0–50, 000 years cal BP. *Radiocarbon* 55(4):1869–1887.
- Rakowski AZ., Krapiec M, Huels M, Pawlyta J., Dreves A, Meadows J. 2015. Increase of radiocarbon concentration in tree rings from Kujawy village (SE Poland) around AD 774–775. *Nuclear Instruments and Methods in Physics Research B* 351:564–568.
- Rakowski AZ, Krapiec M, Huels M, Pawlyta J, Boudin M. 2018. Increase in radiocarbon concentration in tree rings from Kujawy village (SE Poland) around AD 993–994. *Radiocarbon* 60(4):1249–1258. doi: [10.1017/rdc.2018.74](https://doi.org/10.1017/rdc.2018.74)
- Rinn F. 2005. TSAP-Win. Time series analysis and presentation for dendrochronology and related applications. User reference. Heidelberg.
- Rogers KB, Mikaloff-Flecher SE, Bianchi D, Beaulieu C, Galbraith ED, Gnannadesikan A, Hogg AG, Iudicone D, Lintner BR, Naegler T, Reimer PJ, Sarmiento JL, Slater RD. 2011. Interhemispheric gradient of atmospheric radiocarbon reveals natural variability of Southern Ocean wind. *Climate of the Past* 7:1123–1138.
- Suiter M, Polach HA. 1977. Discussion: reporting of ^{14}C data. *Radiocarbon* 19:355–363.
- Usoskin IG, Kromer B, Ludlow F, Beer J, Friedrich M, Kovaltsov GA, Solanki S, Wacker L. 2013. The AD775 cosmic event revisited: the Sun is to blame. *Astron. Astrophys.* 55: L3. doi: [10.1051/0004-6361/201321080](https://doi.org/10.1051/0004-6361/201321080).
- Usoskin IG. 2017. A history of solar activity over millennia. *Living Rev Sol Phys* 14:3. doi: [10.1007/s41116-017-0006-9](https://doi.org/10.1007/s41116-017-0006-9)
- Wang FY, Yu H, Zou YC, Dai ZG, Cheng KS. 2017. A rapid cosmic-ray increase in BC 3372–3371 from ancient buried tree rings in China. *Nature Communications*. doi: [10.1038/s41467-017-01698-8](https://doi.org/10.1038/s41467-017-01698-8).
- Wojdyr M. 2010. Fityk: a general-purpose peak fitting program. *Journal of Applied Crystallography* 43:1126–1128. [10.1107/S0021889810030499](https://doi.org/10.1107/S0021889810030499)